Physicochemical Properties of Nd WIPP Solids

Daniel Olive[1], Marian Borkowski[2], Jean-Francois Lucchini[2], Hnin Khaing[2], Michael Richmann[2], Donald Reed[2], Jeff Terry[1]

[1]Physics Division, BCPS Department, IIT
[2] Los Alamos National Laboratory, Carlsbad Operations

Abstract

The Waste Isolation Pilot Plant (WIPP) located in Southeastern New Mexico is the nation's first licensed and operating permanent repository for transuranic waste. The repository is located in the Salado salt formation at an average depth of 2150 ft. Part of the preparation for recertification of the WIPP site includes the determination of actinide solubility reactions. In order to simplify experimental design and improve the reliability of data multivalent actinides, in this case plutonium and americium, are investigated using an appropriate redox invariant analog, neodymium. Crystals precipitated out of a solution consisting of Generic Weep Brine (GWB) and neodymium were taken to the Advanced Photon Source at Argonne National Laboratory for EXAFS analysis along with neodymium hydroxide, neodymium carbonate, and neodymium hydroxycarbonate standards. Theoretical models of the standards were successfully fit to the data, confirming the validity of the technique. Fitting results on the unknown suggest that Nd substitutes for Ca in a cystalline $Ca(SO_4)$ matrix that precipitates out of the brine solution.

Introduction

In order to ensure the continuing safe operation of the WIPP repository, actinide solubility studies are ongoing. Calculations show that both plutonium and americium are the most important contributors to the potential release scenarios. The solubility and speciation of these multivalent actinides are often investigated by using redox invariant analogs, in this case neodymium. The use of non-radioactive analogs allows for a simplified experimental design and consequently more experimental data is available for inclusion in the long term release models.

The performance assessment calculations for the potential release of trivalent actinides from the WIPP repository salt layer (figure 1) show that their release into the environment is highly unlikely. These calculations are based upon several assumptions about the solubility of Pu(III) and Am(III) in WIPP brine.

To verify the accuracy of the model the solubility of Nd, as an oxidation-invariant analog, in simulated WIPP brines (table 1) was tested. Precipitates of a different solid phase than initially present in the brine are thought to control neodymium solubility. EXAFS analysis is used to characterize this precipitate.

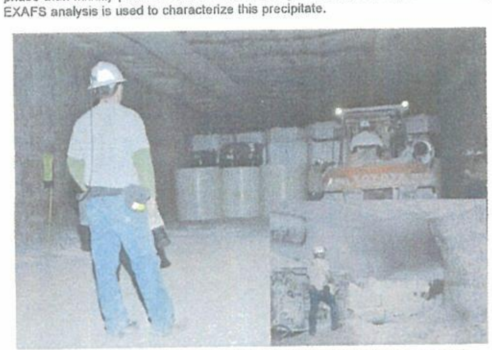

Figure 1: Workers 2150 ft. below ground in the WIPP repository. Placing containers of transuranic waste into the repository (main). Miner excavating salt to form a cavern (inset). The salt layer extends more than 1000 ft. above and below the level of the repository.

Component	NaCl	$MgCl_2$	Na_2SO_4	NaBr	$Na_2B_4O_7$	KCl	$CaCl_2$	LiCl
GWB [M]	2.874	0.953	0.166	0.025	0.037	0.473	0.013	0.004

Table 1: Composition of the GWB simulated WIPP brine.

Experimental Setup

The solubility of Nd(III), as an oxidation-state invariant analog for Pu(III) and Am(III) was measured by adding 10^{-2} M neodymium in hydrochloric acid to simulated WIPP brines under varying pC_{H+} (between 6.5 and 10.5) and carbonate concentrations (from 0 to 0.01M) with the temperature held constant at room temperature. The pC_{H+} is simply pH with a brine dependent constant added on, for GWB this constant is 1.23 ±0.01. The carbonate is expected to form naturally in the repository as carbon dioxide generated from the microbial degradation of organic waste dissolves in the brine and reacts with the MgO packed along with the waste to act as a barrier. Calcium and iron(II) also present in the repository are also expected to form carbonates. Each experiment was allowed to equilibriate for 200-350 days, after which the precipitate was recovered. The primary reactions thought to control Nd solubility are summarized below.

$$Nd^{3+} + OH^- \rightleftharpoons NdOH^{2+}$$
$$Nd^{3+} + 2OH^- \rightleftharpoons Nd(OH)_2^{1+}$$
$$Nd^{3+} + CO_3^{2-} \rightleftharpoons NdCO_3^{1+}$$
$$Nd^{3+} + 2CO_3^{2-} \rightleftharpoons Nd(CO_3)_2^{1-}$$
$$Nd(OH)_3(s) \rightleftharpoons Nd(OH)_2^{1+} + OH^-$$
$$Nd_2(CO_3)_3(s) \rightleftharpoons Nd_2(CO_3)_2^{2+} + CO_3^{2-}$$
$$NdCO_3OH(s) \rightleftharpoons NdCO_3^{1+} + OH^-$$
$$Nd(OH)_2^{1+} + B(OH)_4^{1-} \rightleftharpoons Nd(OH)_2B(OH)_4(s) \text{ or } NdBO3(s) + 3\ H_2O$$
$$Nd(OH)_2B(OH)_4(s) + B(OH)_4^{1-} \rightleftharpoons Nd(OH)_2[B(OH)_4]_2^{1-}$$

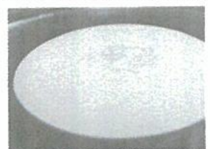

Figure 2: Crystal precipitates remaining after solubility experiment.

The results of the solubility experiment with the carbonates are shown below in figure 3. The equilbrium point is approached from points of oversaturation and undersaturation. During oversaturation, an excess amount of soluble Nd (dissolved in HCl) is added to the brine, which precipites out to reach equilibrium. For undersaturation, a solid is dissolved in solution until equilibrium is achived.

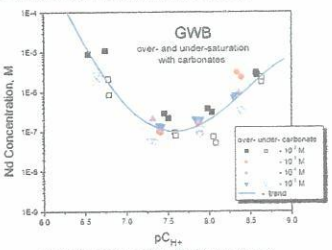

Figure 3: Results of Nd solubility experiment.

However, the solids recovered after the experiment were in the form of large single crystal needles (figure 2), unlike the hydroxide, carbonate, or hydroxycarbonate used in the experiment. In order to characterize the precipitate samples they were sent to the Advanced Photon Source at Argonne National Laboratory for EXAFS analysis (figure 4).

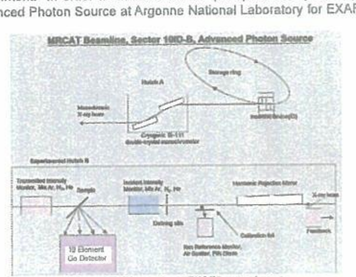

Figure 4: Schematic of EXAFS experiment.

Results and Discussion

Serving as potential candidates for the unknown as well as test cases for the anlytical technique were three standards: Neodymium hydroxide, neodymium carbonate, and neodymium hydroxycarbonate. The actual data gathered by the EXAFS experiment consist of x-ray absorbtion, shown in figure 5.

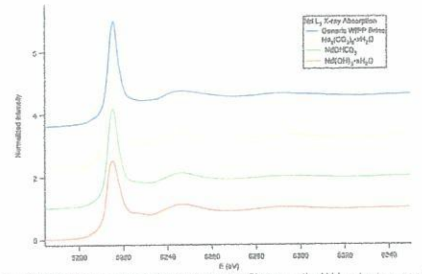

Figure 5: Normalized x-ray absorbtion vs. energy. Shown are the Nd L_3 edge jumps and characteristic EXAFS oscillations after the edge.

The oscillations are caused as changing de Broglie wavelengths of the photoelectrons, created by the x-rays, constructivley and destructivley interfere as they scatter off of neighboring atoms. By taking the Fourier transform of these oscillations (figure 6) we can use the EXAFS equation to model scattering in momentum space.

$$\chi(k) = S_0^2 \sum_i \frac{N_j}{kR_j^2} |f_j(k,r)| e^{-2k^2\sigma_j^2} e^{-2R_j/\lambda(k)} \sin(2kR_j + \delta_j(k,r))$$

Where we have grouped elements of the same type and distance into shells, and averaged over all angles, the structural information for the j^{th} shell is given by N_j, R_j, and σ_j^2, which represent the coordination number, average distance, and mean square variation in distance (the Debye-Waller factor) respectively.

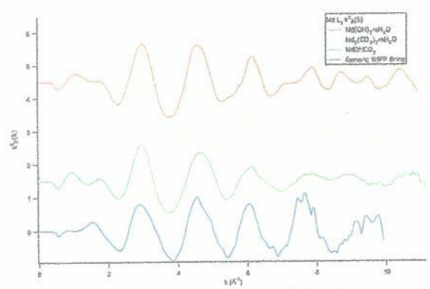

Figure 6: Data for each sample, in $k^3\chi(k)$ vs. k.

Using information about their crystal structures, models were created of the three standards. ARTEMIS software, running FEFF6 was used to calculate theoretical scatting paths based on those models. The paths were fit to the data, and the resultant parameters of best fit were used to extract physical details from each system (fig. 7)

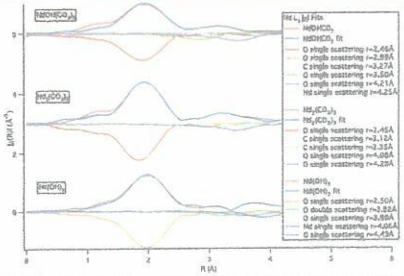

Figure 7: Fitting results of the three standards. Comparison of the reverse Fourier transforms of the EXAFS data for each of the standards with their respective fits (top half of each group) along with the paths whose sums comprise the fit (bottom half of each group) reflected about the x-axis for clarity.

The unknown sample was fit to the same models as the standards, but produced no match. A gypsum, $Ca(SO_4)$, crystal structure (figure 9) was then modeled, with Nd substituting Ca as the scattering center, the results of that fit are shown in figure 8.

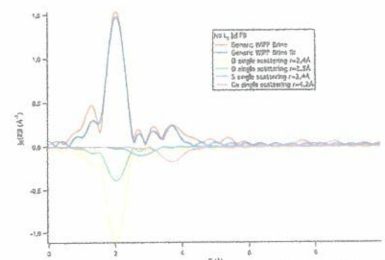

Figure 8: Fitting results of the unknown using gypsum's crystal strucure. Comparison of the reverse Fourier transforms of the EXAFS data to the fit based on a gypsum matrix (top half) along with the paths whose sums comprise the fit (bottom half) reflected about the x-axis for clarity.

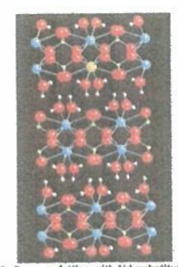

Figure 9: Gypsum lattice with Nd substitution at core scattering center. C2/c space group, a=6.284 A, b=15.20 A, c=6.5230 A, β=127.410 °. Ca in blue, Nd in orange, O in red, H in pink.

Path	R(Å)	N	σ^2
Neodymium hydroxycarbonate			
O	2.45±0.01	6.0±0.6	0.01
O	2.98±0.10	0.63±0.67	0.001
C	3.27±0.030	3.7±1.1	0.001
O	3.48±0.035	3.3±1.3	0.005
O	4.21±0.033	9.4±3.1	0.01
Nd	4.25±0.050	3.4±2.0	0.01
Neodymium carbonate			
O	2.45±0.012	7.2±0.97	0.006
C	3.12±0.050	3.2±1.7	0.005
C	3.25±0.23	1.3±1.9	0.005
O	4.08±0.036	11±4.2	0.007
O	4.28±0.057	5.8±3.1	0.001
Neodymium hydroxide			
O	2.50±0.011	7.3±0.7	0.002
O	3.98±0.050	2.8±1.6	0.001
O-O	3.82±0.084	25±17	0.002
Nd	4.06±0.050	4.8±2.6	0.006
O	4.49±0.041	4.9±2.9	0.001
Unknown in gypsum matrix			
O	2.53±0.02	4.15±0.65	0.002
O	2.54±0.035	1.5±0.74	0.005
S	3.37±0.23	0.82±1.3	0.008
Ca	4.34±0.09	1.0±1.5	0.005

Table 2: Parameters for best fit paths. Uncertainties determined by what change is necessary to double R-value, the goodness-of-fit

Conclusion and References

The continued operation of the WIPP repository is contingent upon recertification, part of which is based on models of actinide behavior in the environment. The predictions made by these models of the solubility limiting solid phase lack physicality. An unexpected Nd substitution in a gypsum matrix was discovered using EXAFS analysis of the precipitate remaining after Nd solubility studies in simulated WIPP brine. Clearly additional study is required to determine the primary reactions and kinetics associated with actinides in the WIPP environment.

Booyens, J., V. Ichharam, Zeitschrift fur Kristallographie. 217, 6-10. (2002)
Borkowski, M., J-F. Lucchini, S. Ballard, M. Richmann, D. Reed, D. Olive, J. Terry. in preparation
Dexpert, H., and P. Caro, Mat. Res. Bul. 9, 1577 (1974)
Ravel, B., M. Newville, J. Synchrotron Rad., 12, 537, (2005)
Ravel, B., J. Synchrotron Rad., 8, 322, (2001)
Rehr, J. J., and R. C. Albers, Phys. Rev. B. 41, 8139, (1990)
Rehr, J. J., and R. C. Albers, Rev. Mod. Phys. 72, 621, (2000)
Sayers, D. E., E. A. Stern, and F. W. Lytle, Phys. Rev. Lett. 27, 1204, (1971)
Tareen, J. A. K., T. R. Narayanan, and K. V. Krishnamurty, J. Crystal Growth, 49, 761 (1980)
Zachariasen, W. H., Acta Cryst., 1, 265 (1948)

LA-UR- 08-2288

Approved for public release;
distribution is unlimited.

Title:	Physicochemical Properties of Nd WIPP Solids
Author(s):	Dan Olive Marian Borkowski Jean-Francois Lucchini Michael K. Richmann Hnin Khaing Donald T. Reed Jeff Terry
Intended for:	Poster presentation at the May 4-8, 2008 Argonne Advanced Photon Source Users Meeting

Los Alamos
NATIONAL LABORATORY
EST.1943

Los Alamos National Laboratory, an affirmative action/equal opportunity employer, is operated by the Los Alamos National Security, LLC for the National Nuclear Security Administration of the U.S. Department of Energy under contract DE-AC52-06NA25396. By acceptance of this article, the publisher recognizes that the U.S. Government retains a nonexclusive, royalty-free license to publish or reproduce the published form of this contribution, or to allow others to do so, for U.S. Government purposes. Los Alamos National Laboratory requests that the publisher identify this article as work performed under the auspices of the U.S. Department of Energy. Los Alamos National Laboratory strongly supports academic freedom and a researcher's right to publish; as an institution, however, the Laboratory does not endorse the viewpoint of a publication or guarantee its technical correctness.

Form 836 (7/06)